Evolution of Microstructure and Microtexture in Friction Stir Welded Oxide Dispersion Strengthened Steel

Brad Baker

Luke Brewer, Terry McNelley, E.S.K. Menon
Naval Postgraduate School, Monterey, CA

This work in part was performed under the auspices of the U.S. Department of Energy by Lawrence Livermore National Laboratory under Contract DE-AC52-07NA27344.

Motivation – Material Requirements

Advanced structural materials are needed for first wall/containment vessels for advanced energy designs.

Oxide dispersion strengthened (ODS) ferritic-martensitic steels are potential candidates (MA956/957, PM1000/2000, 12/14YWT).

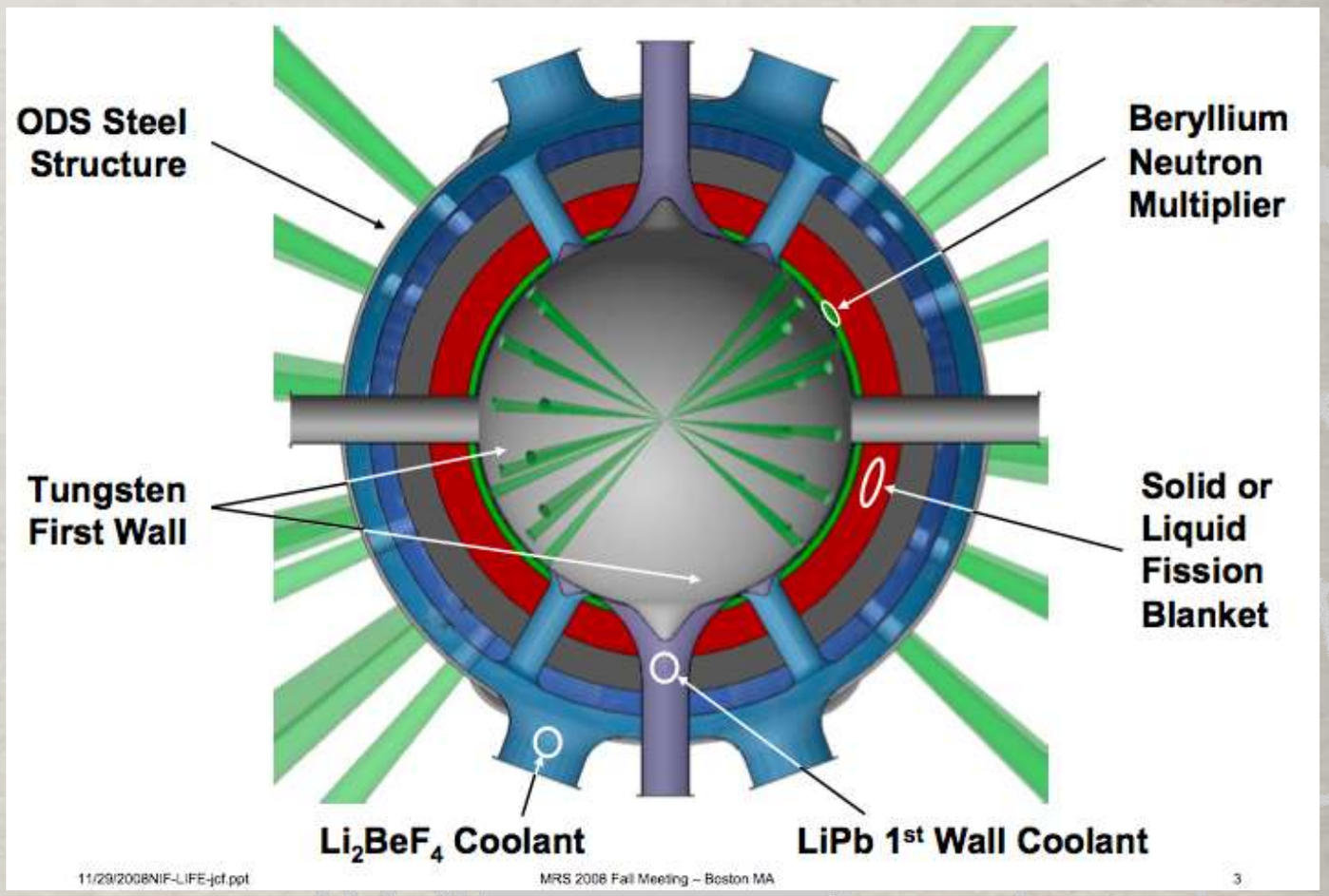

Depiction of the fusion chamber for LIFE
Farmer, LLNL, 2008.

However, traditional fusion welding techniques for ODS steels are not suitable due to agglomeration of oxide particles during welding.

Motivation – Joining of ODS Steels

- High hardness
- High strength
- Low ductility
- BCC ferritic structure

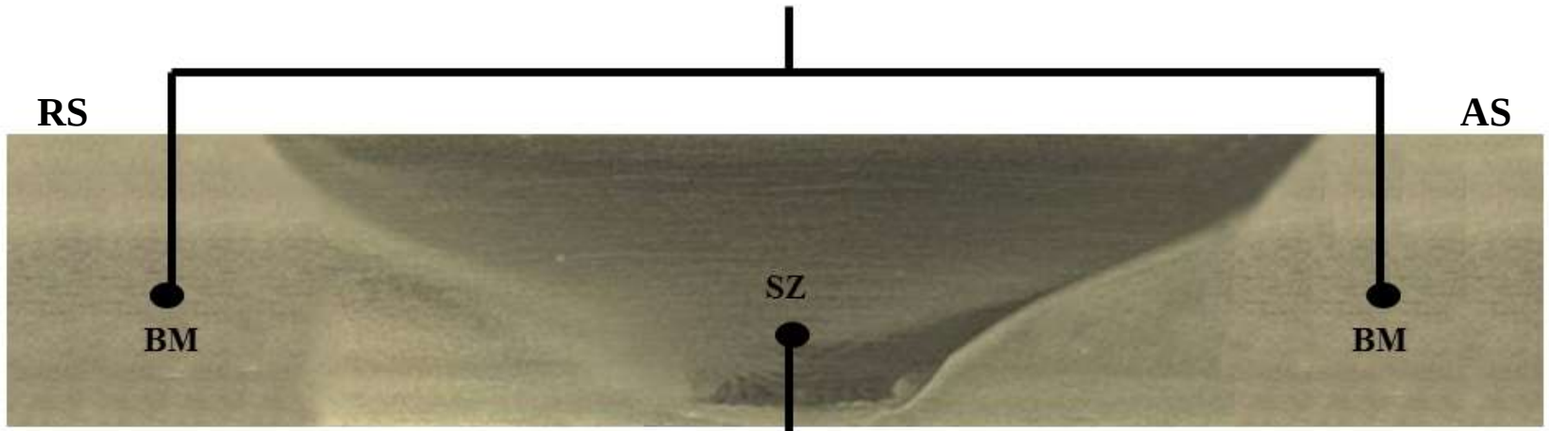

- Undermatched weld
- No porosity
- Reduced hardness
- Reduced strength
- Improved ductility
- BCC ferritic structure

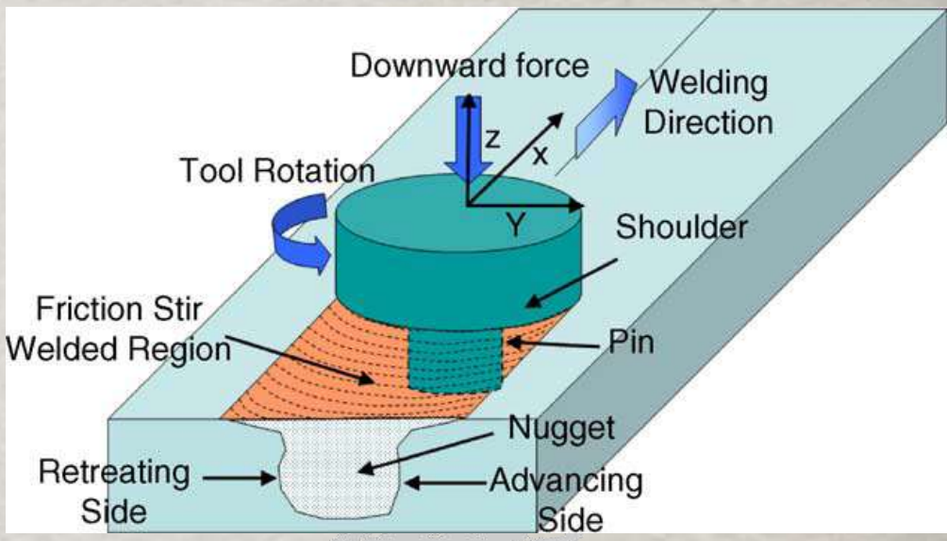

Friction Stir Welding (FSW) process
Mishra, 2005

FSW parameters varied:

Tool rotational rate (ω)
Tool traverse rate (ν)

<u>Objective:</u>
Determine the processing-microstructure-material property relationships by analyzing the evolution of microstructure and microtexture in friction stir welded ODS steel.

How does grain size vary?
What is the microtexture? Does it change?
What happens to the dispersed oxides?

Experimental Techniques

- **Metallographic preparation**
  - Transverse cross sections prepared using SiC papers, aluminum oxide polishing solutions, colloidal silica solution, and finally electropolished in 10% perchloric acid in ethanol at -23°C.

- **Scanning Electron Microscopy (SEM)**
  - Zeiss Neon 40 field emission SEM at 20 keV and 60 μm objective aperture.

- **Electron backscatter diffraction (EBSD)**
  - EDAX-TSL OIM 6.0 system with a Hikari camera at 20 keV using 60 μm objective aperture and probe current of approximately 1 nA.
  - Denoised using cleanup functions of grain dilation and grain confidence index standardization.
  - Minimum area dimensions of 150x300 μm equating to a minimum of 2000 grains.

- **Energy dispersive x-ray spectroscopy (EDS)**
  - Same SEM at 12 keV.
  - 23x17 μm sections (5000x) counted for 200 seconds with 6% dead time equating to 188 live seconds typically resulting in peaks of 10000 counts.
  - Al-K (1.486 keV) and Y-L (1.922 keV) analyzed with ZAF corrections applied for qualitative determination of Y-Al-O phases YAM and YAG.

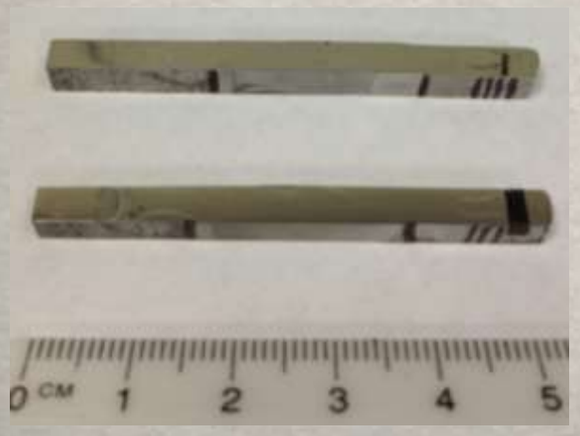

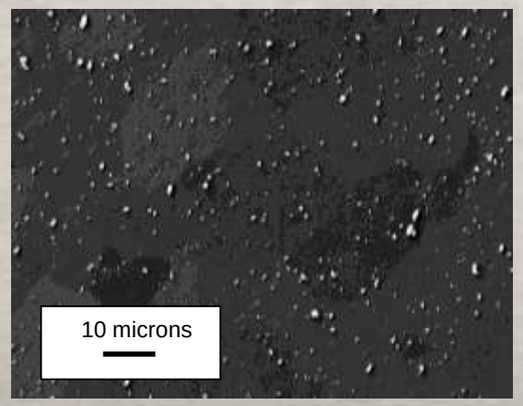

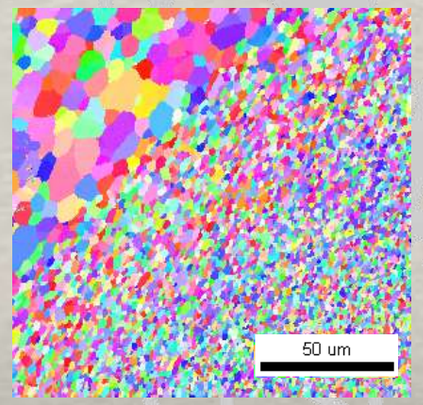

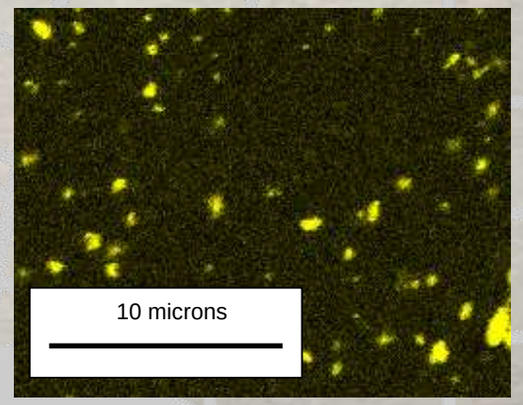

Grain Growth in the SZ

Grains are significantly coarsened in the SZ compared to the starting grain size of 0.89 μm in the BM.

Grain size in the stir zone increase from 4.2 μm to 12.5 μm at the highest heat input.

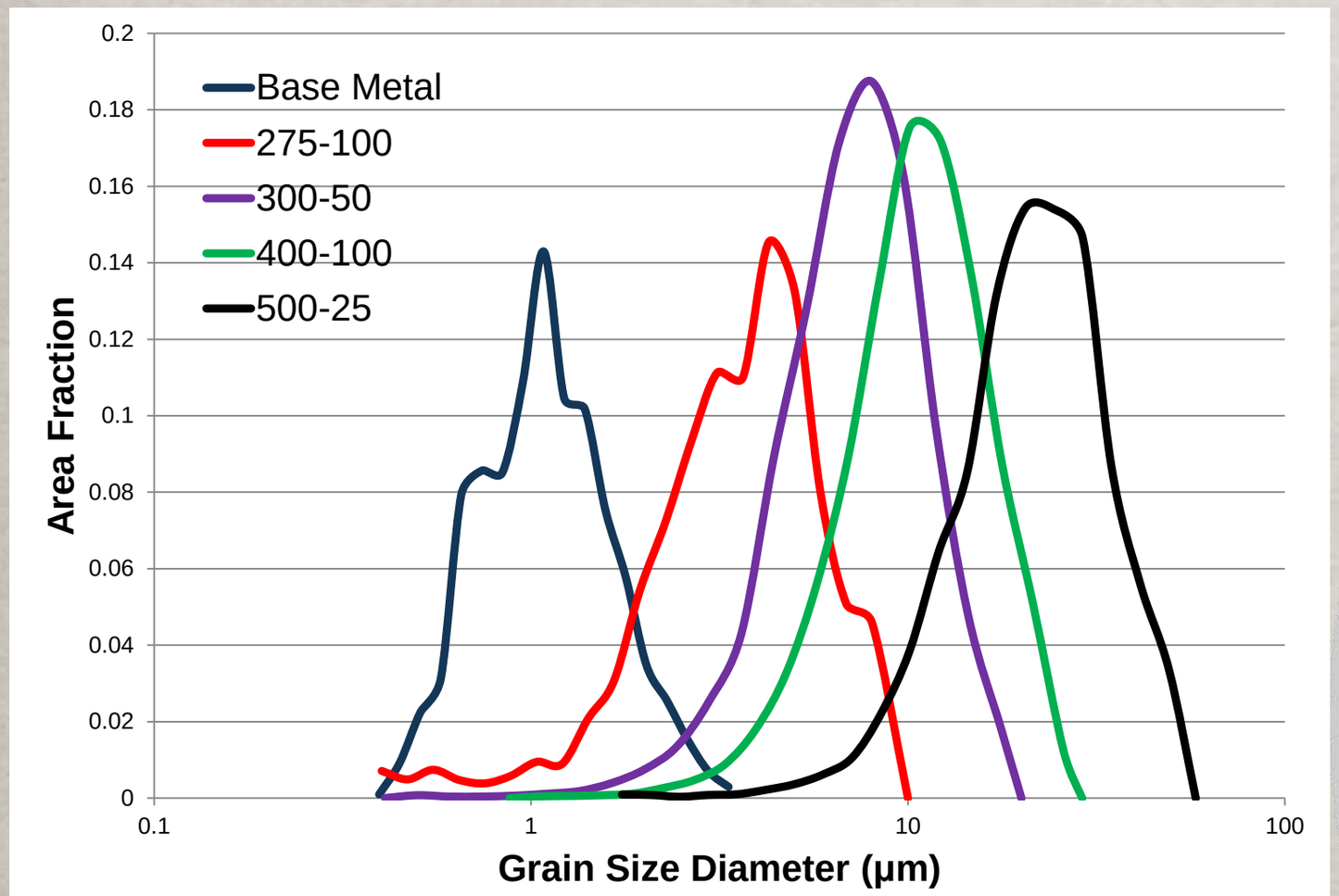

Increasing heat input →

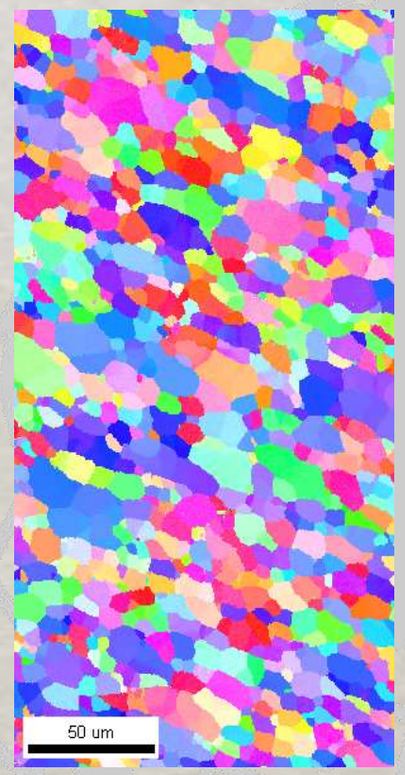

400/100

500/25

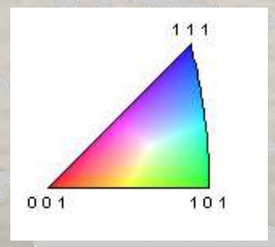

Persistence of Low Angle Grain Boundaries

Although the SZ does contain mostly equiaxed grains, there is a significant amount (approximately 20%) of **low angle grain boundaries** (LAGB defined as 1-10 degrees) indicating continuous dynamic recrystallization.

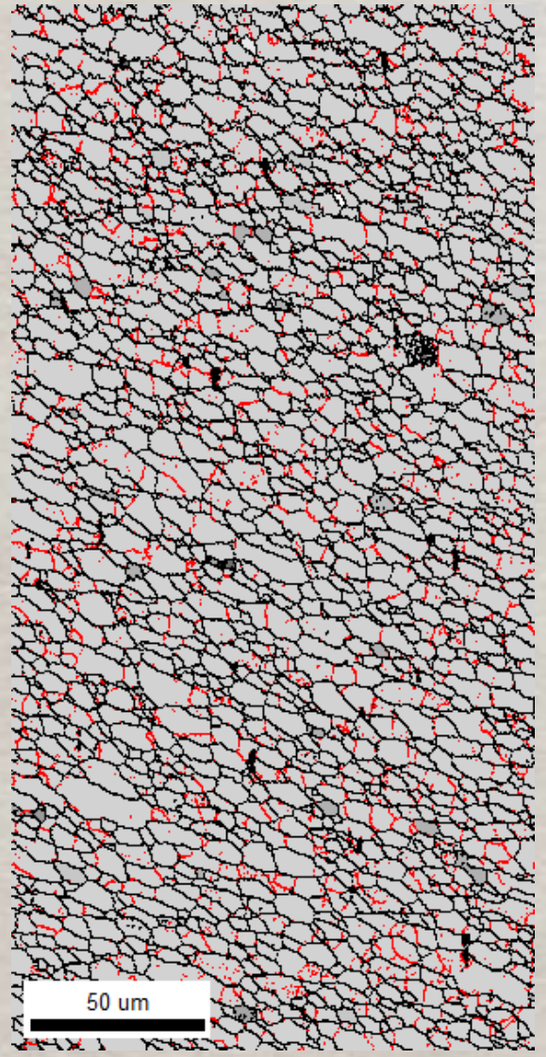

300/50

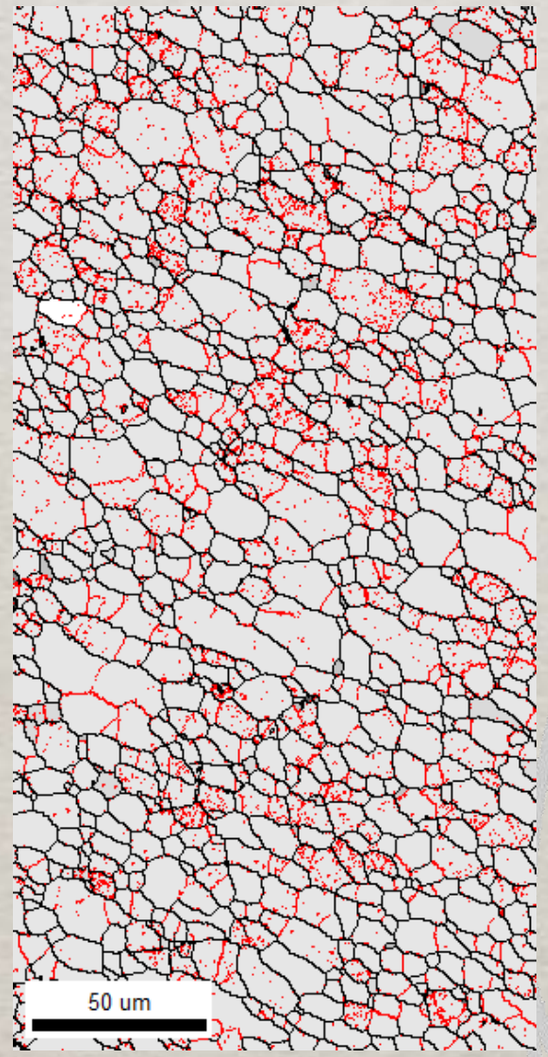

400/100

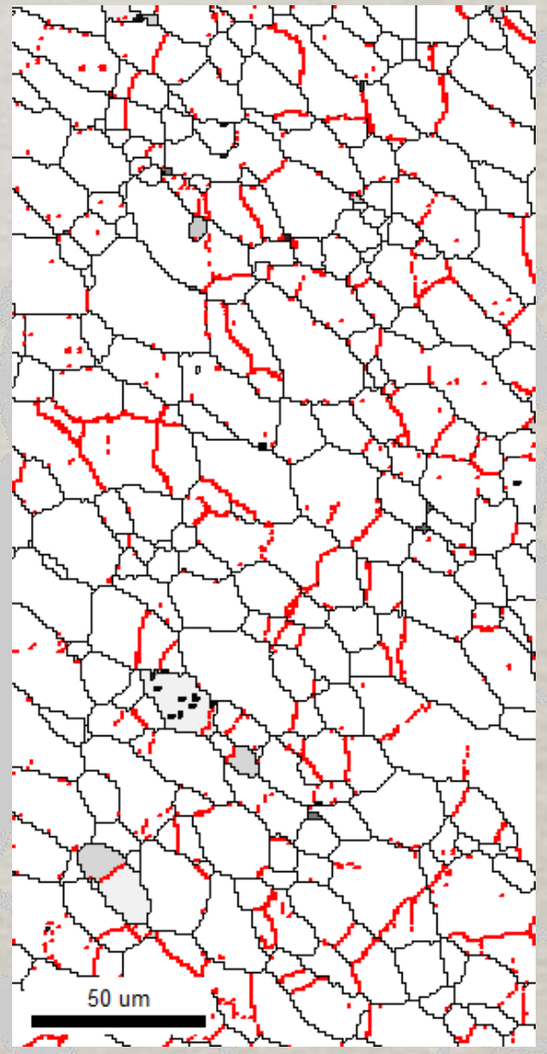

500/25

Texture in the SZ

The shearing plastic deformation of FSW produces a persistent simple shear texture in the SZ for all welding conditions that closely resembles theoretical shear textures.

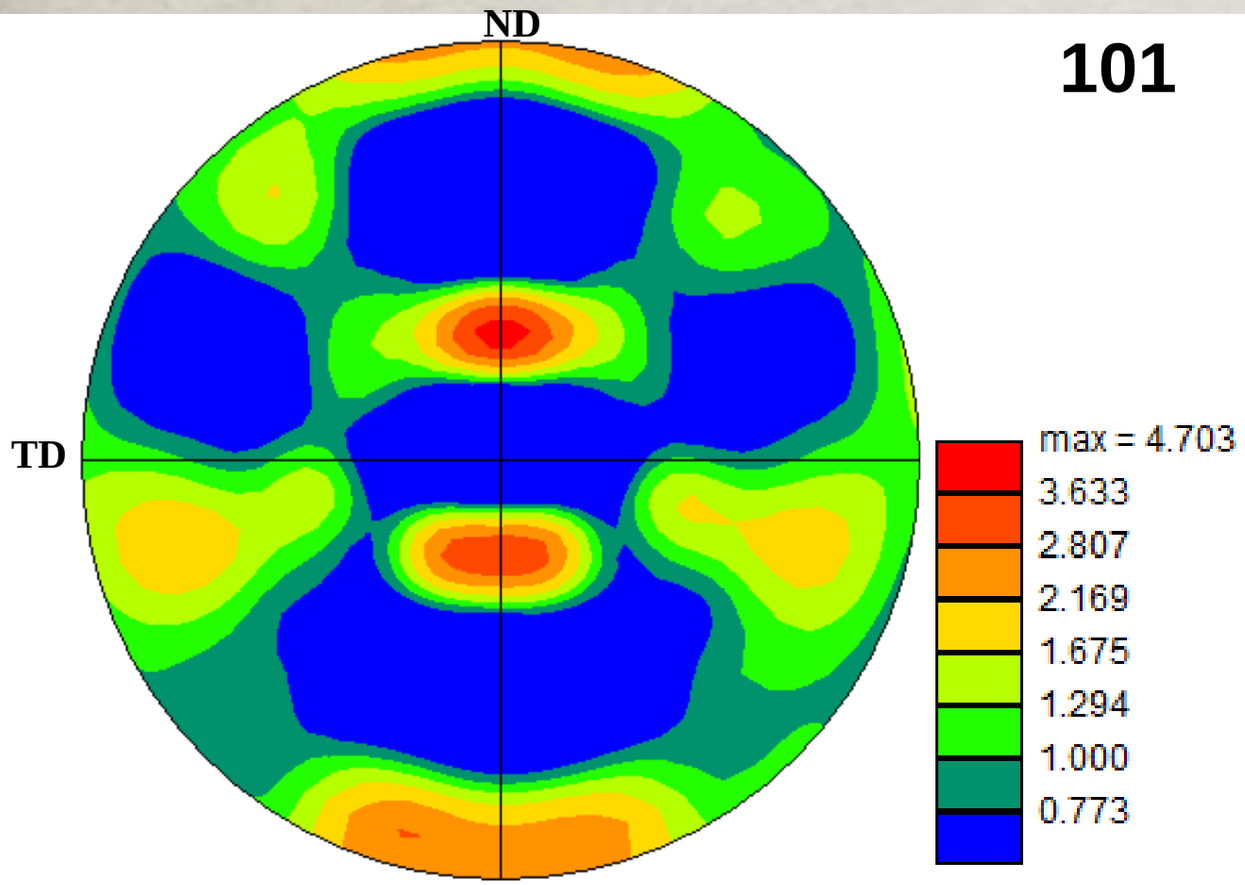

Base metal rolled texture

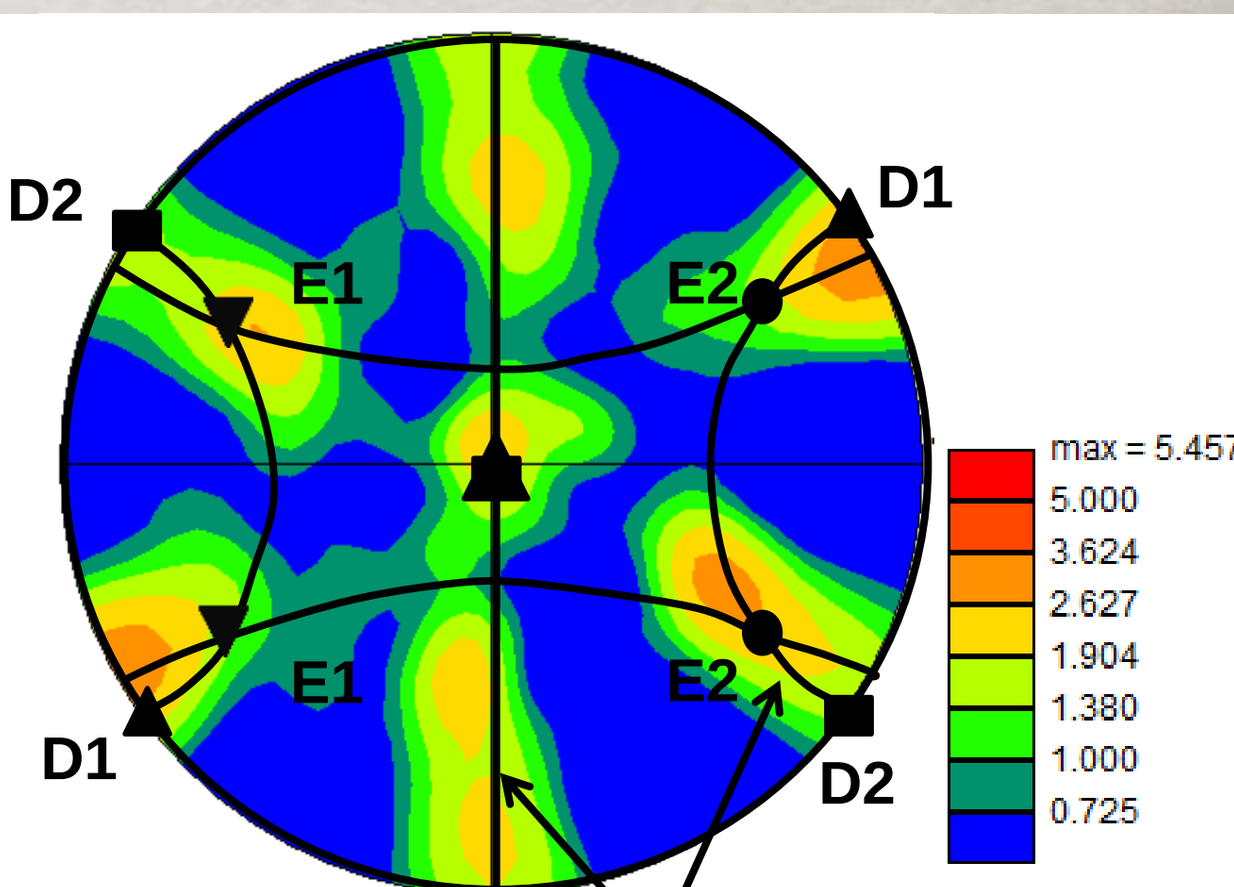

SZ simple shear texture in the shear plane overlaid with ideal torsional texture from *Baczynski, 1996.*

Persistence of Texture in the SZ

The simple shear texture persists for all FSW conditions examined (from low heat input to high input) indicating a deformation based texture.

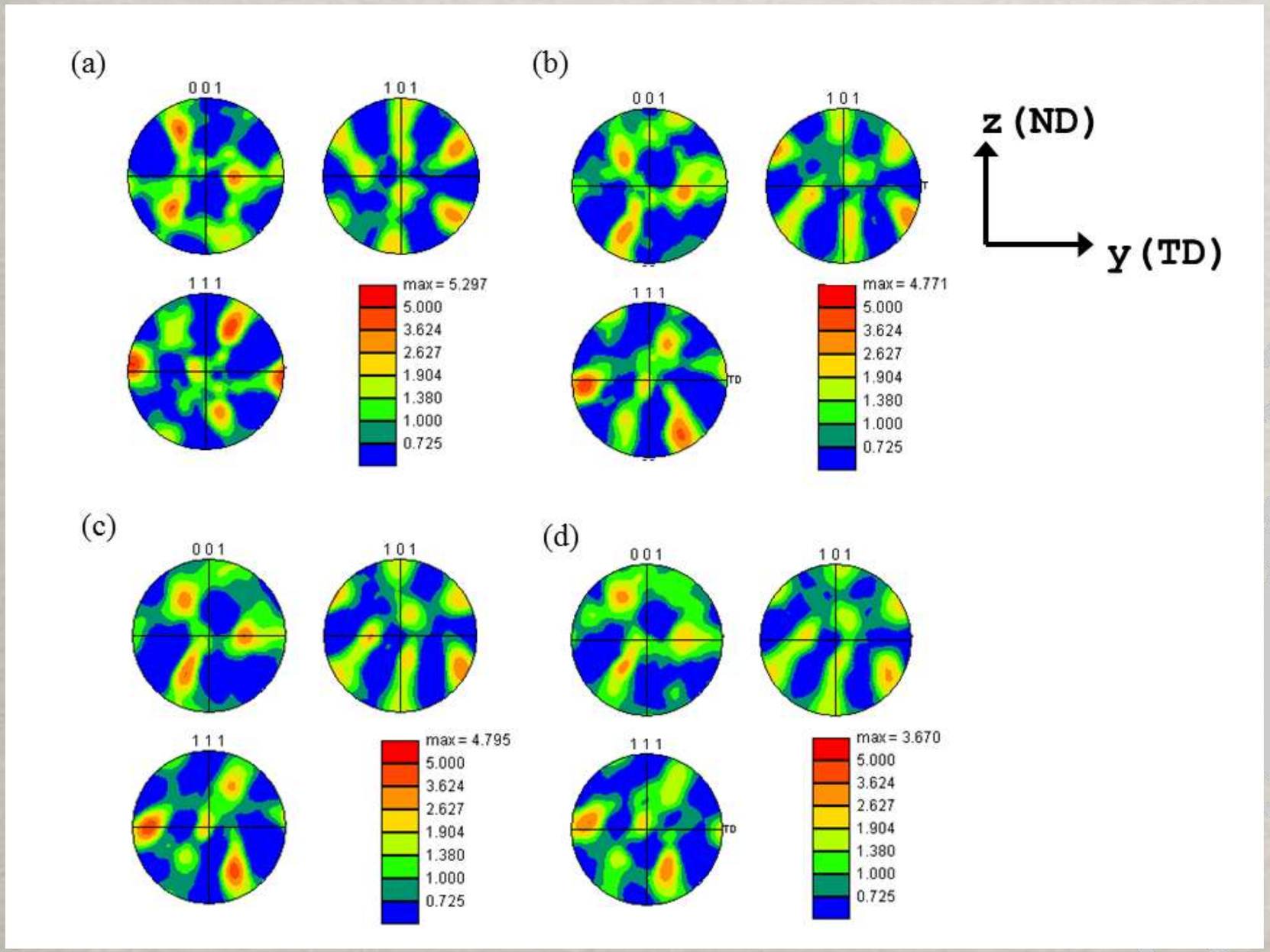

(a) 275 RPM/100 MMPM (lowest heat input)

(b) 300 RPM/50 MMPM

(c) 400 RPM/100 MMPM

(d) 500 RPM/25 MMPM (highest heat input)

Grain Growth Across the Weld Nugget

Grain growth across the weld nugget is not symmetric and is highly dependent on FSW parameters.

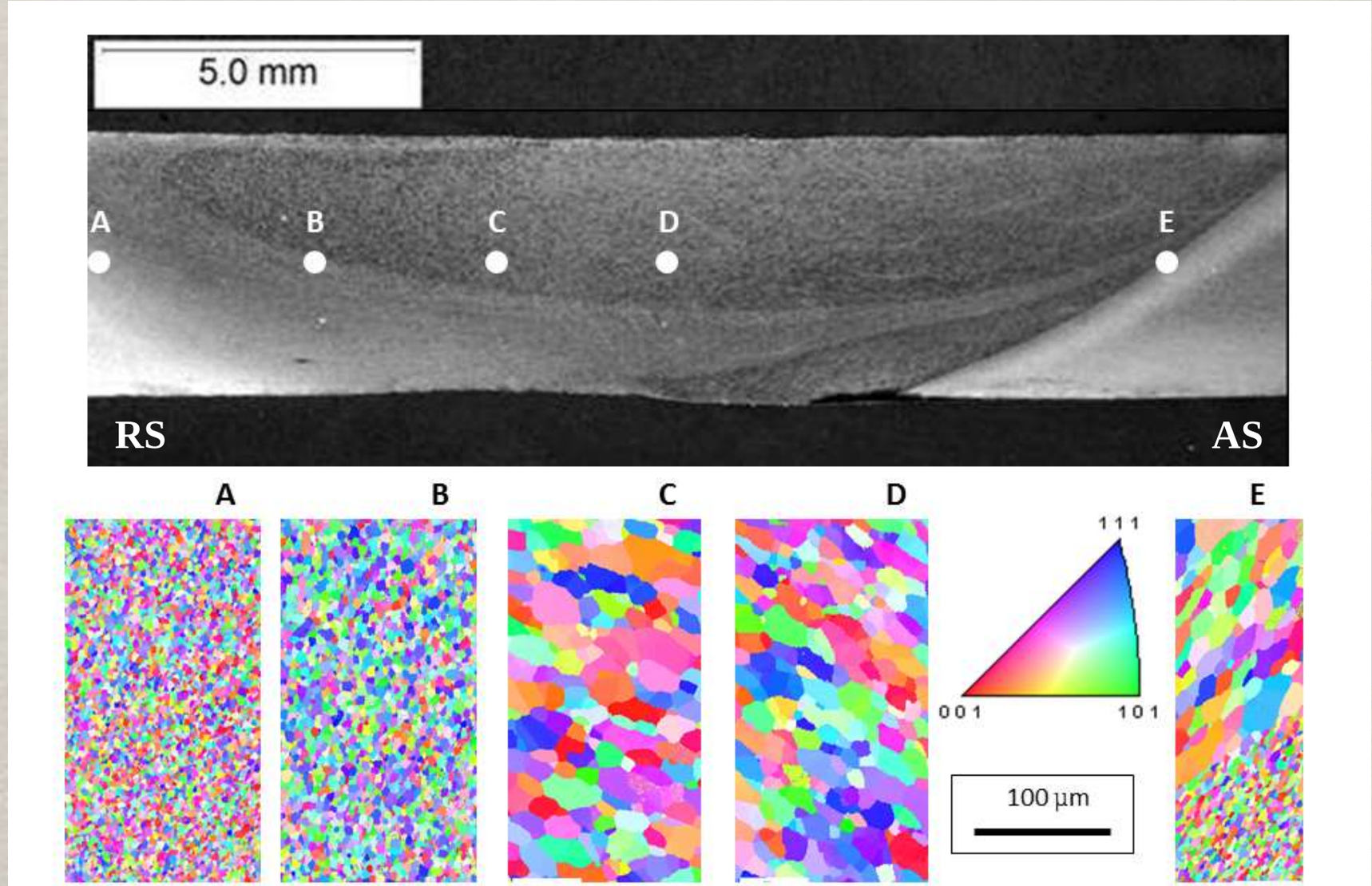

Schematic profile of grain growth across the weld nugget for the highest heat input condition (500 RPM/25 MMPM)

TMAZ Gradients

Strong gradients in grain size were observed on the advancing side (AS) of each weld. The magnitude of the gradients was also a function of heat input. These gradients did not exist on the retreating side (RS).

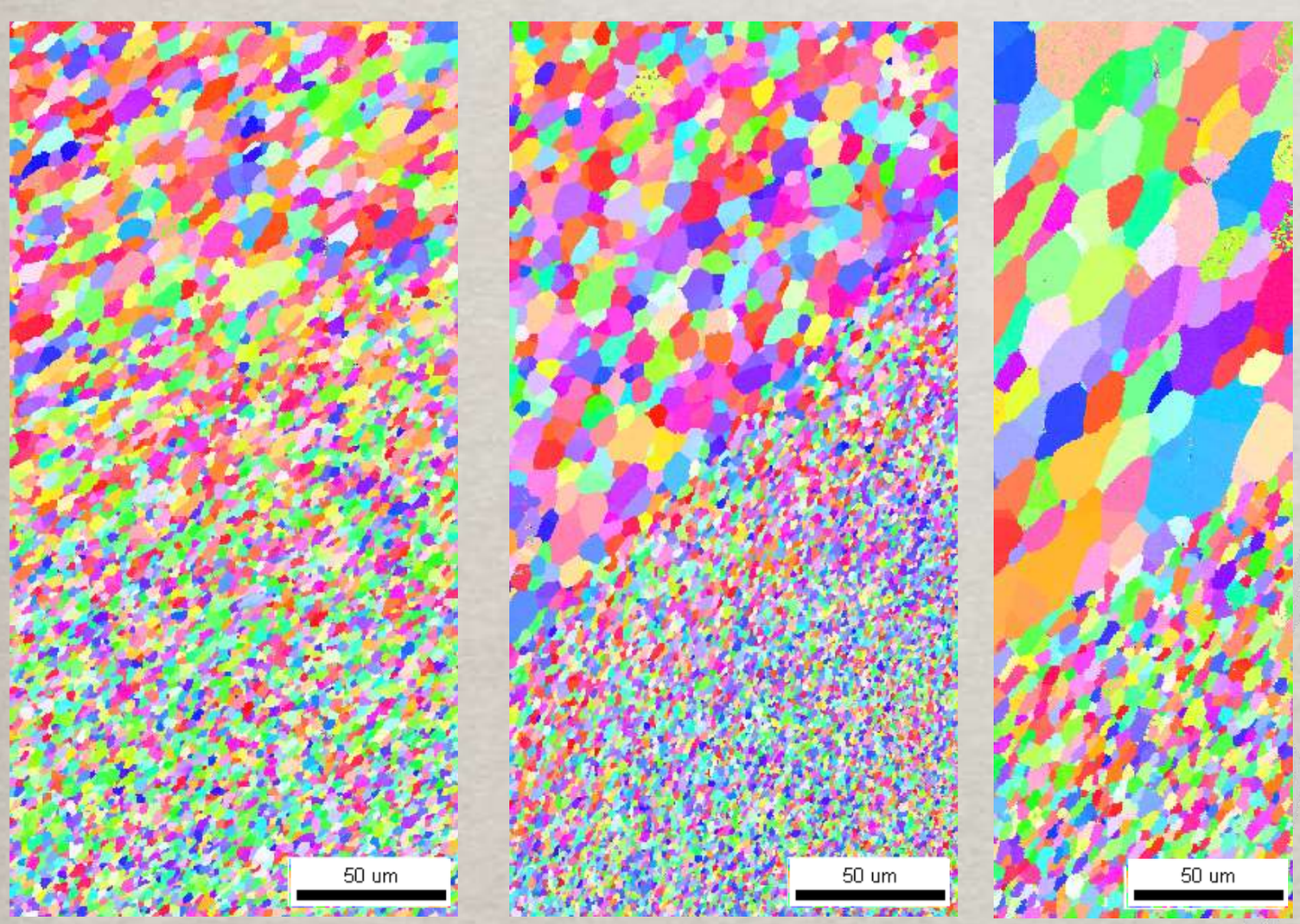

400/100 300/50 500/25

Increasing heat input →

These gradients are hypothesized as potential failure locations due to strain localization.

These gradients prompted further analysis of the AS TMAZ which has shown similar gradients for:

- Hardness
- Oxide particle coarsening
- Residual stress

Microstructure to Material Property Relationships

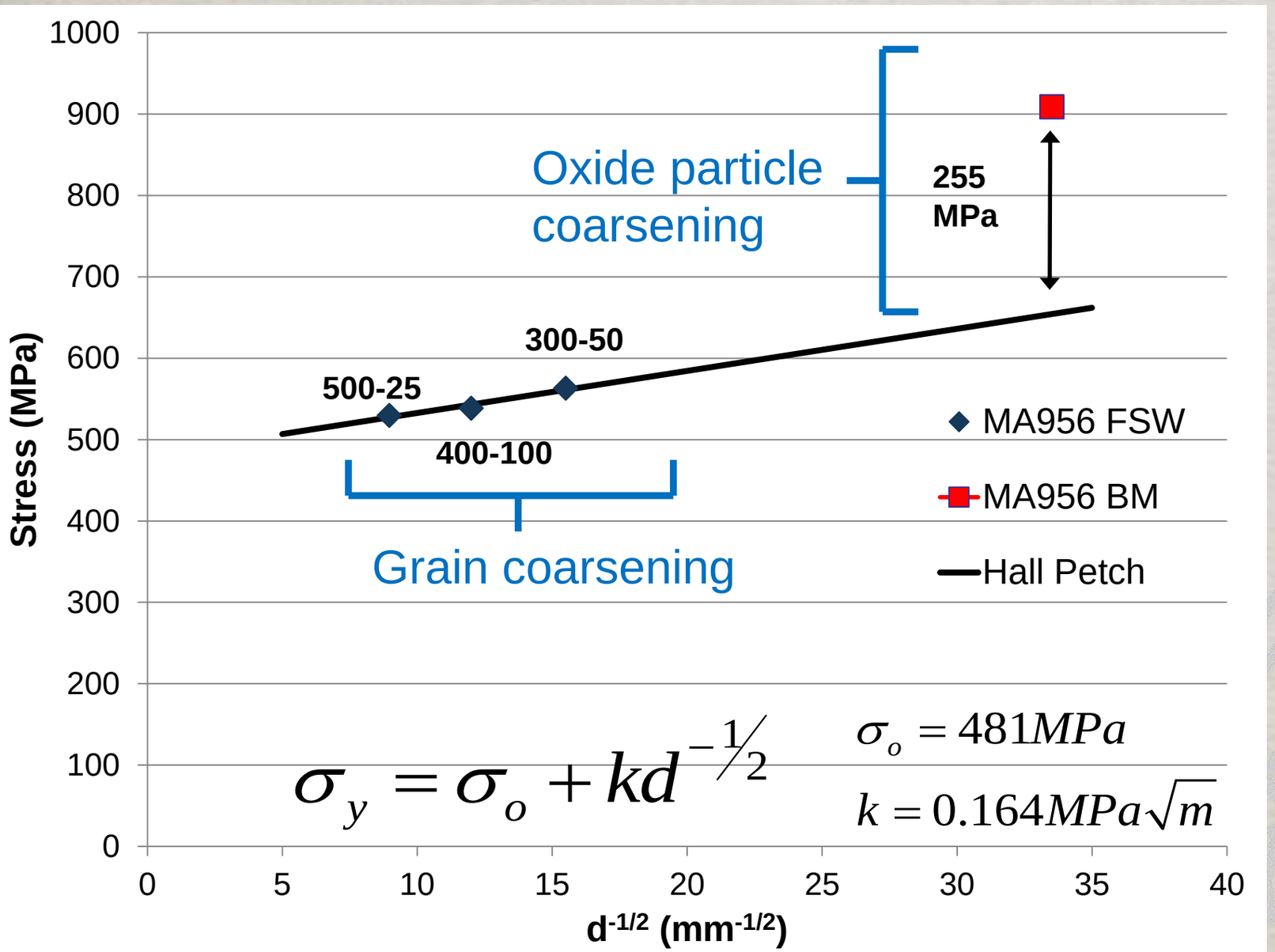

FSW of ODS steel causes:

- Grain coarsening
- Oxide particle coarsening

Both of which contribute to a reduction in strength.

EBSD and EDS have helped prove established material property relationships.

Qualitative Oxide Particle Distribution

Heat input from FSW causes oxide particle coarsening in the SZ due to continued phase transformation in the Al_2O_3-Y_2O_3 system. Complex nano scale Y-Al-O particles are formed during the powder metallurgy process which then grow to micro scale particles during FSW. Higher HI conditions produce greater particle coarsening.

Scanning electron microscopy imagery:

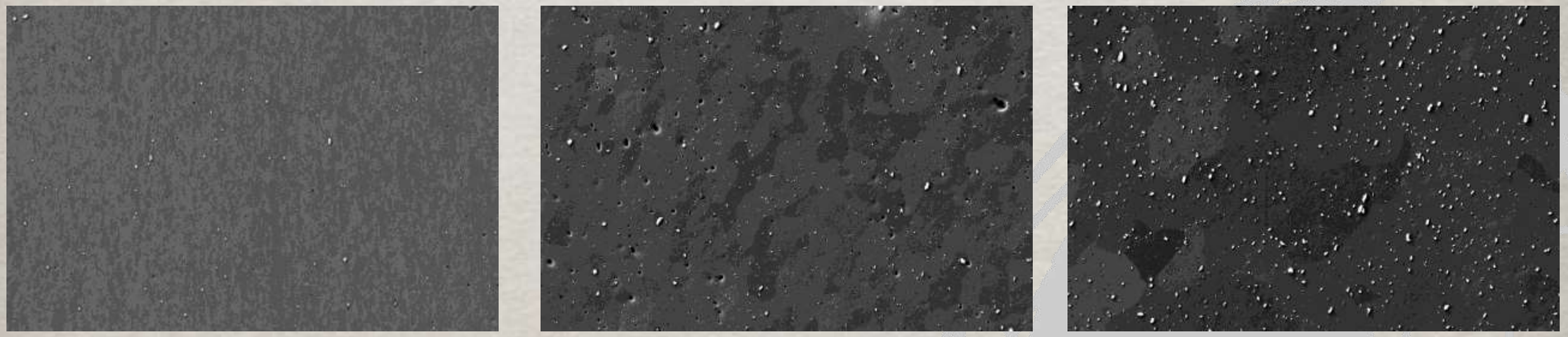

Increasing HI

Energy dispersive x-ray spectroscopy (yellow-Yttrium, purple-Titanium):

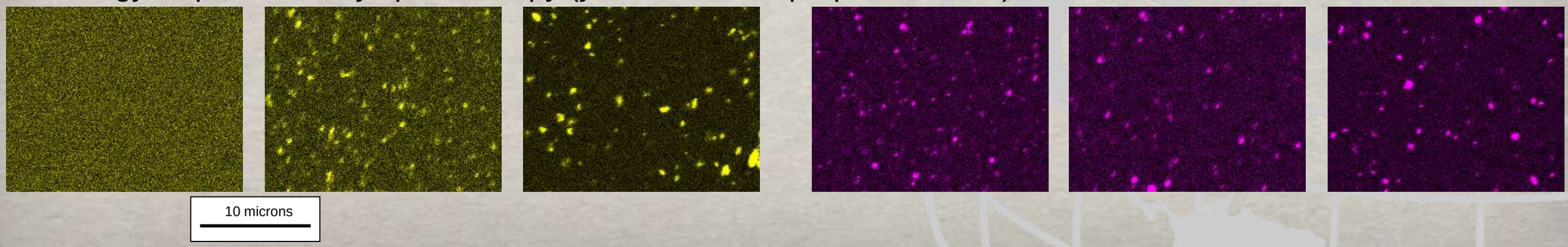

Summary

Properties
- High hardness
- High strength
- Low ductility
- BCC ferritic structure

Microstructure
- Very fine grains
- Very fine oxide particles
- Rolled texture

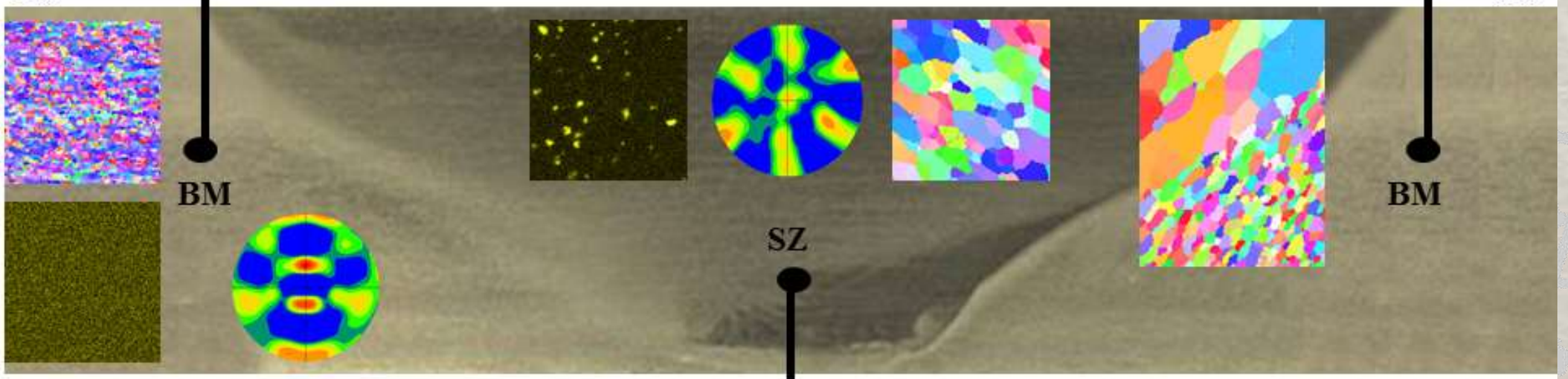

Properties
- Undermatched weld
- No porosity
- Reduced hardness
- Reduced strength
- Improved ductility
- BCC ferritic structure

Microstructure
- Coarsened grains
- Coarsened oxide particles
- BCC shear texture
- Sharp transition on AS only

Backup Slides

Oxide Particle Phase Determination

Oxide	Chemical Reaction	Formation Temperature Range
YAM ($Y_4Al_2O_9$)	$2Y_2O_3 + Al_2O_3 \rightarrow Y_4Al_2O_9$	900C-1100C
YAP ($YAlO_3$)	$2Y_2O_3 + 2Al_2O_3 \rightarrow 4YAlO_3$	1100C-1250C
YAG ($2Y_3Al_5O_{12}$)	$3Y_2O_3 + 5Al_2O_3 \rightarrow 2Y_3Al_5O_{12}$	1400C-1600C

Yttrium Aluminum Garnet (YAG)

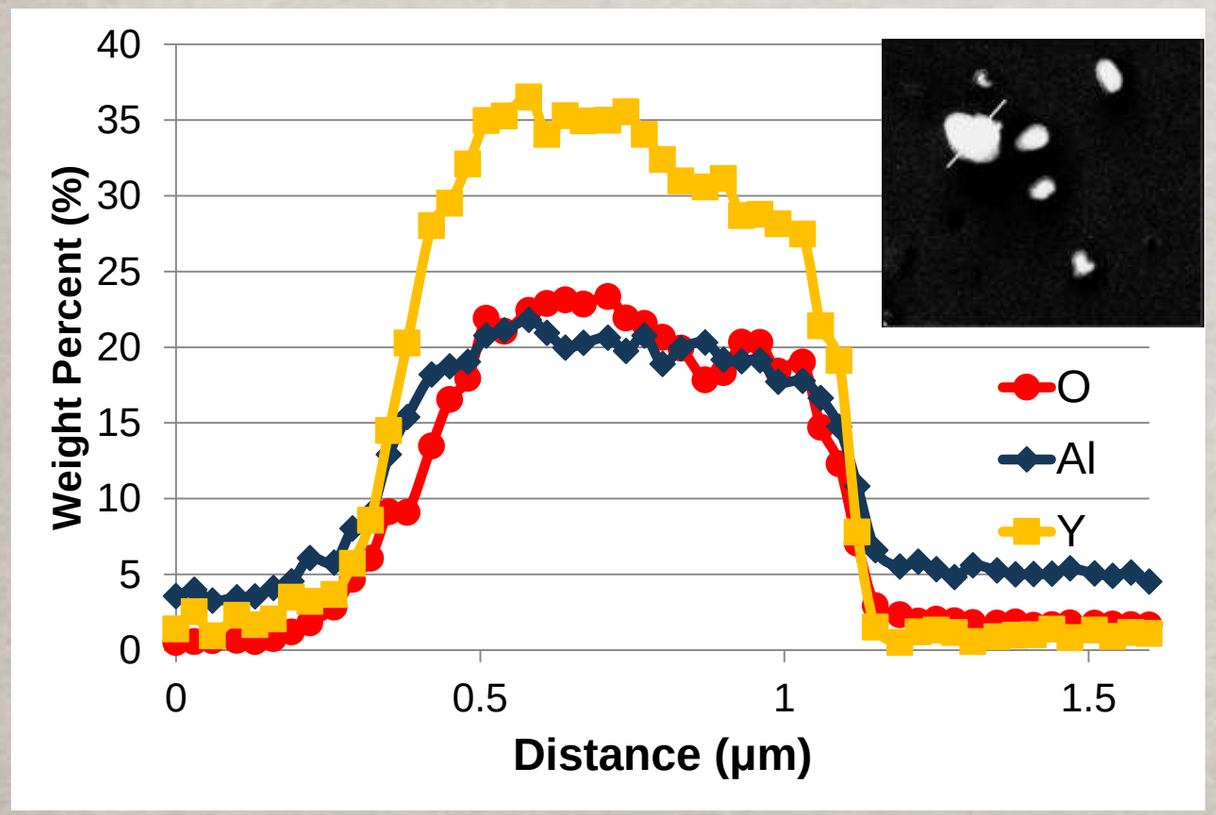

Yttrium Aluminum Monoclinic (YAM)

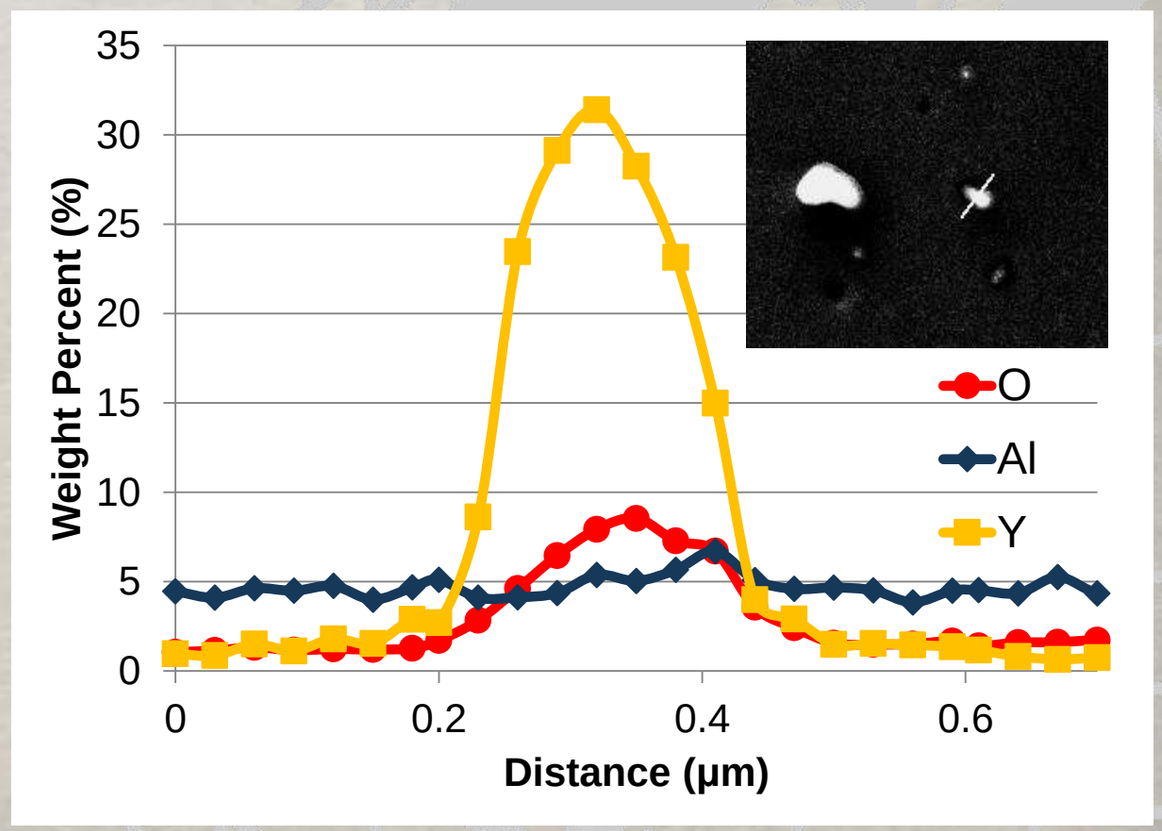

Oxide Particle Phase Determination

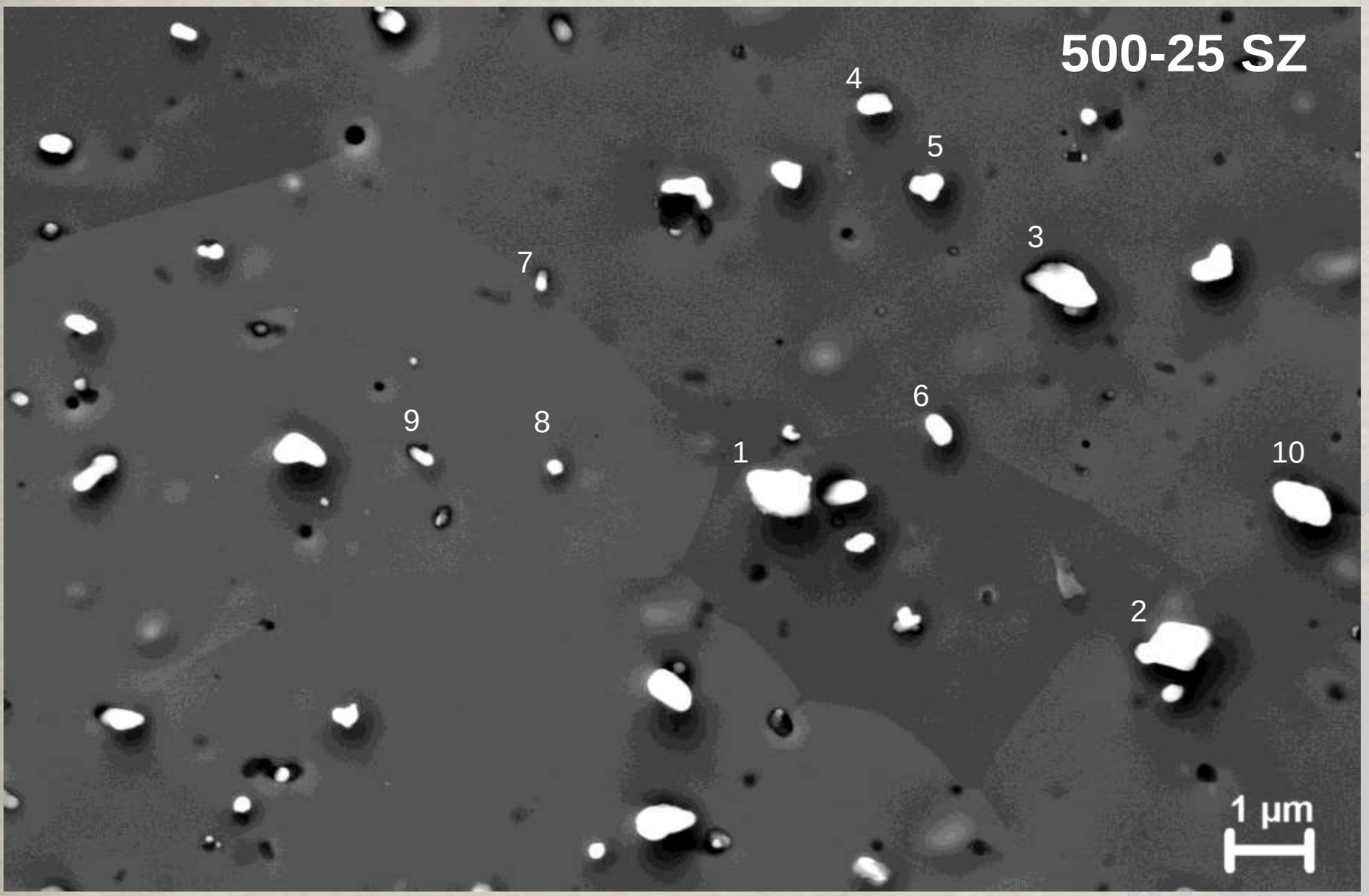

#	$IR_{Y/Al}$ (YAM=1.671) (YAP=1.208) (YAG=0.814)	$AR_{Y/Al}$ (YAM=2) (YAP=1) (YAG=0.6)	Phase
1	0.672	0.535	YAG
2	0.720	0.570	YAG
3	0.694	0.551	YAG
4	0.750	0.592	YAG
5	0.627	0.501	YAG
6	0.659	0.525	YAG
7	0.796	0.626	YAG
8	0.808	0.635	YAG
9	2.803	2.057	YAM
10	0.826	0.648	YAG

IR = Intensity Ratio (raw intensity comparison)
AR = Atom Ratio (calculated by EDAX Genesis)

Oxide Particle Phase Determination

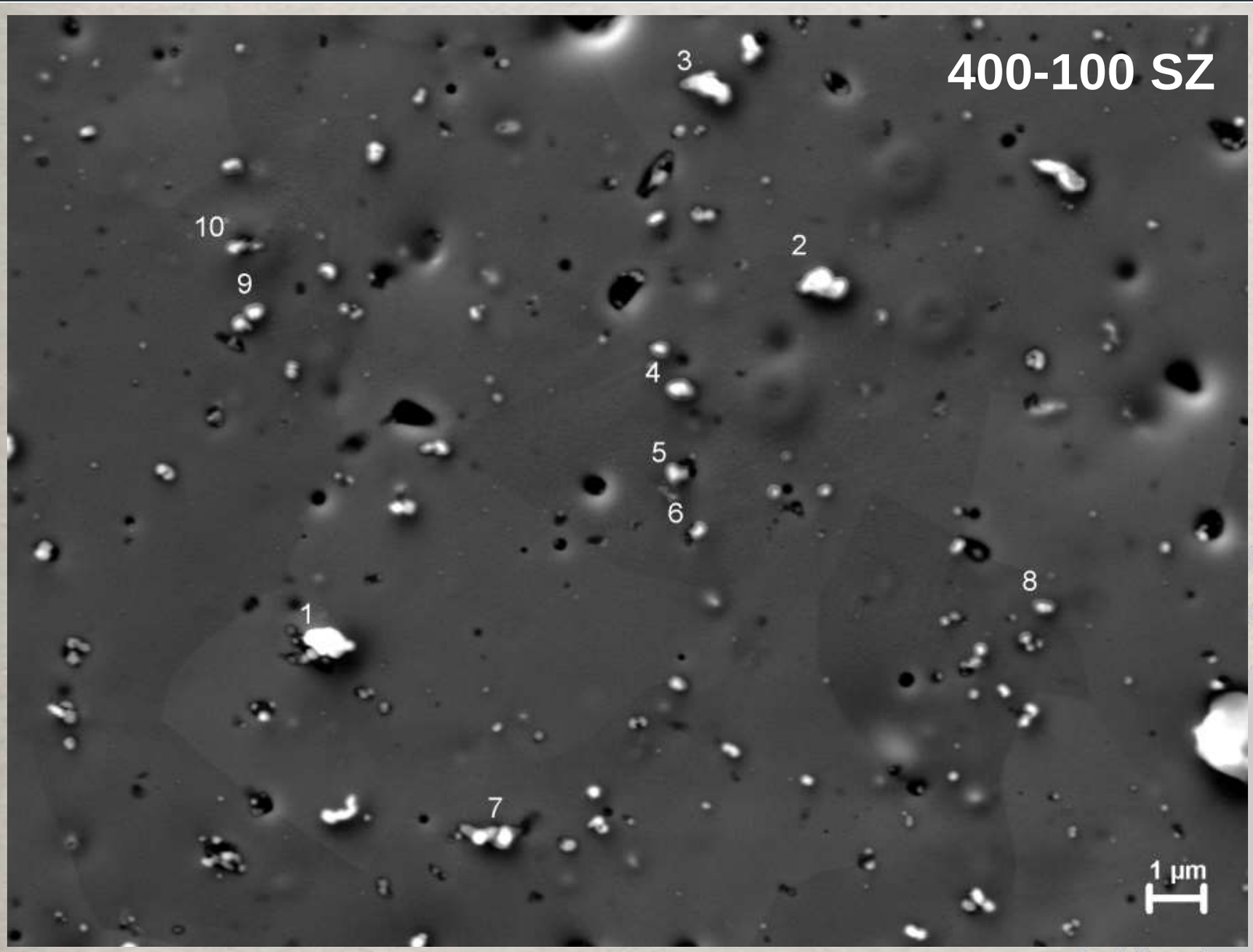

#	$IR_{Y/Al}$ (YAM=1.671) (YAP=1.208) (YAG=0.814)	$AR_{Y/Al}$ (YAM=2) (YAP=1) (YAG=0.6)	Phase
1	0.075	0.084	*
2	0.156	0.181	*
3	0.231	0.274	*
4	0.716	0.920	YAG
5	0.490	0.613	YAG
6	0.497	0.622	YAG
7	0.404	0.499	YAG
8	0.626	0.798	YAG
9	0.538	0.678	YAG
10	0.658	0.839	YAG

* Indeterminate

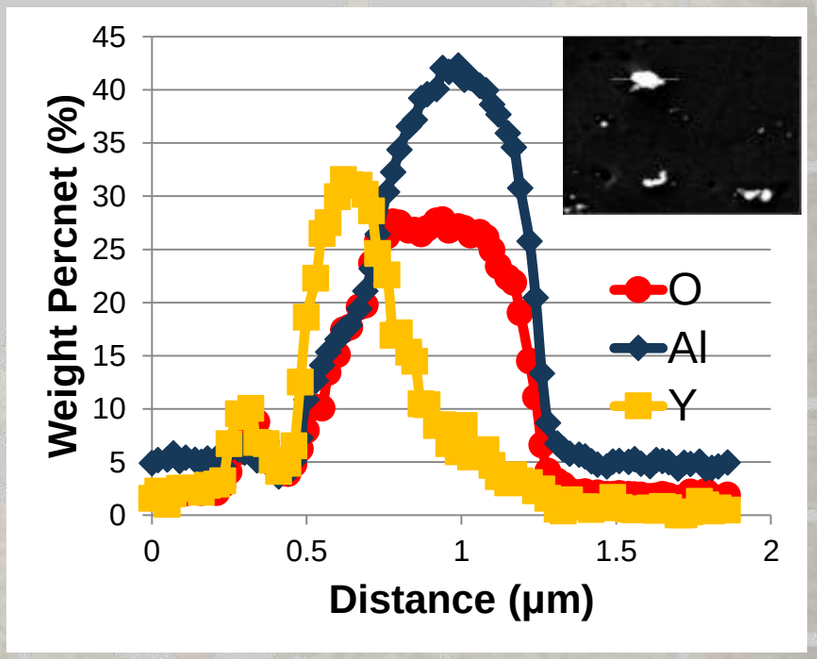

IR = Intensity Ratio (raw intensity comparison)
AR = Atom Ratio (calculated by EDAX Genesis)

Small Angle X-ray Scattering (SAXS) Results

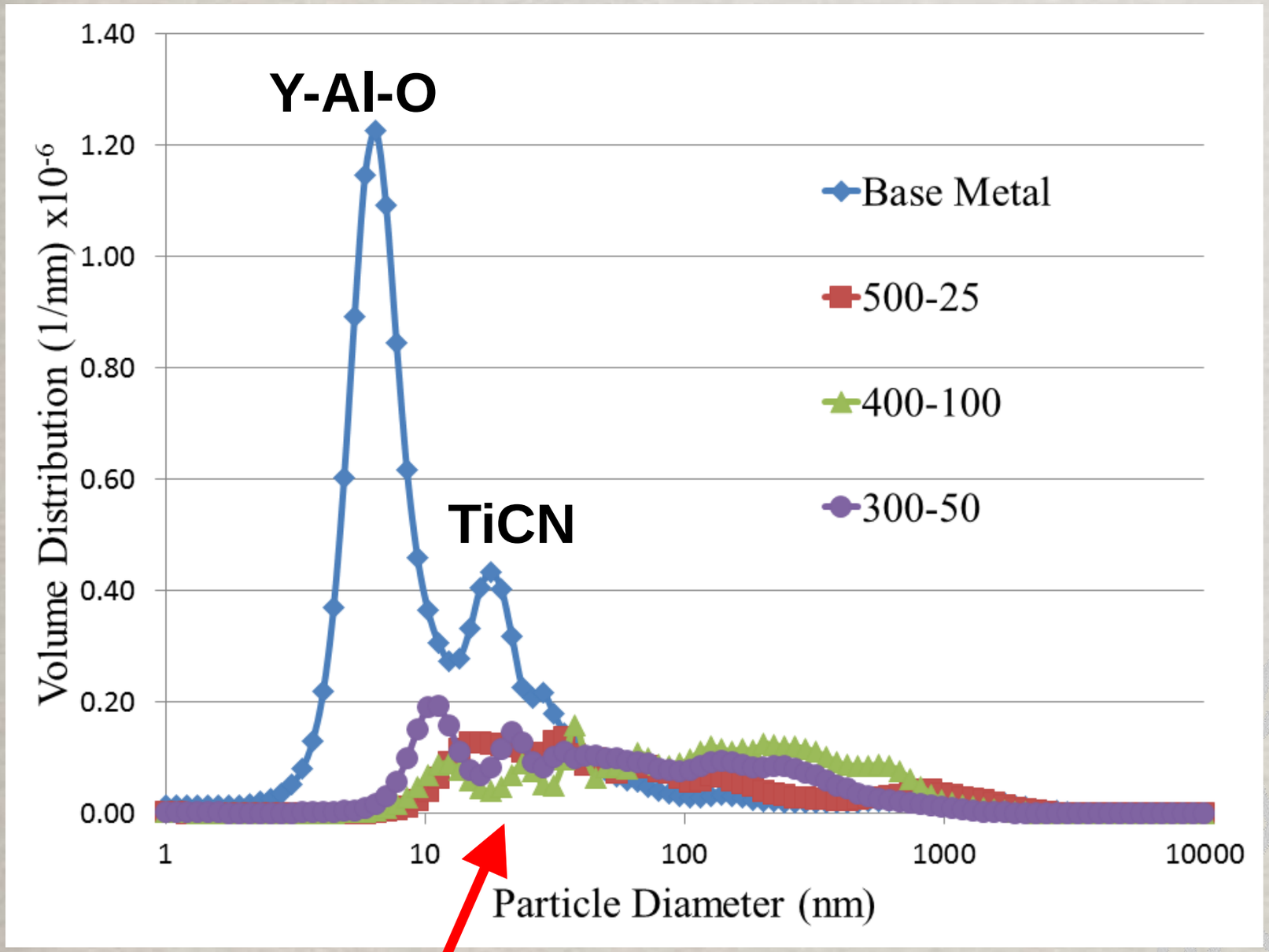

SAXS results show:

- 2 peaks in the BM
- Virtually no nm size particles in the SZ

In all FSW conditions, almost all nm sized particles are gone.